US-FT/7-01
June, 2001

The contribution of off-shell gluons to the structure functions F_2^c and F_L^c and the unintegrated gluon distributions

A.V. Kotikov

Bogoliubov Laboratory of Theoretical Physics
Joint Institute for Nuclear Research
141980 Dubna, Russia

A.V. Lipatov

Department of Physics
M.V. Lomonosov Moscow State University
119899 Moscow, Russia

G. Parente

Departamento de Física de Partículas
Universidade de Santiago de Compostela
15706 Santiago de Compostela, Spain

N.P. Zotov

D.V. Skobeltsyn Institute of Nuclear Physics
M.V. Lomonosov Moscow State University
119899 Moscow, Russia

Abstract

We calculate the perturbative parts of the structure functions F_2^c and F_L^c for a gluon target having nonzero transverse momentum squared at order α_s. The results of the double convolution (with respect to the Bjorken variable x_B and the transverse momentum) of the perturbative part and the unintegrated gluon densities are compared with HERA experimental data for F_2^c. The contribution from F_L^c structure function ranges $10 \div 30\%$ of that of F_2^c at the kinematical range of HERA experiments.

PACS number(s): 13.60.Hb, 12.38.Bx, 13.15.Dk

1 Introduction

Recently there have been important new data on the charm structure function (SF) F_2^c, of the proton from the H1 [1, 4] and ZEUS [2, 3] Collaborations at HERA, which have probed the small-x_B region down to $x_B = 8 \times 10^{-4}$ and $x_B = 2 \times 10^{-4}$, respectively. At these values of x_B, the charm contribution to the total proton SF, F_2^p, is found to be around 25%, which is a considerably larger fraction than that found by the European Muon Collaboration at CERN [5] at larger x_B, where it was only $\sim 1\%$ of F_2^p. Extensive theoretical analyses in recent years have generally served to confirm that the F_2^c data can be described through perturbative generation of charm within QCD (see, for example, the review in Ref. [6] and references therein).

In the framework of DGLAP dynamics [7, 8] there are two basic methods to study heavy flavour physics. One of them [9] is based on the massless evolution of parton distributions and the other [10] on the boson-gluon fusion process. There are also interpolating schemes (see Ref. [11] and references therein). The present HERA data [1, 2, 3, 4] for the charm SF F_2^c are in good agreement with the predictions from Ref. [10].

We note, however, that perhaps more relevant analyses of the HERA data, where the x_B values are quite small, are those based on BFKL dynamics [12] (see discussions in the review of Ref. [13] and references therein), because the leading $ln(1/x_B)$ contributions are summed. The basic dynamical quantity in BFKL approach is the unintegrated gluon distribution $\varphi_g(x, k_\perp^2)$ (f_g is the (integrated) gluon distribution multiplied by x_B and $k_\perp$ is the transverse momentum)

$$f_g(x_B, Q^2) \;=\; \int^{Q^2} \frac{dk_\perp^2}{k_\perp^2} \, \varphi_g(x_B, k_\perp^2) \qquad (\text{hereafter } q^2 = -Q^2,\ k^2 = -k_\perp^2\ ), \tag{1}$$

which satisfies the BFKL equation.

We define the Bjorken variables

$$x_B = Q^2/(2pq) \quad \text{and} \quad x = Q^2/(2kq), \tag{2}$$

for lepton-hadron and lepton-parton scattering, respectively, where p^μ and k^μ are the hadron and the gluon 4-momentums, respectively, and q^μ is the photon 4-momentum.

Notice that the integral is divergent at the lower limit and so it leads to the necessity to consider the difference $f_g(x_B, Q^2) - f_g(x_B, Q_0^2)$ with some nonzero Q_0^2 (see discussions

in Sect. 3), i.e.

$$f_g(x_B,Q^2) \;=\; f_g(x_B,Q_0^2) + \int_{Q_0^2}^{Q^2} \frac{dk_\perp^2}{k_\perp^2}\, \varphi_g(x_B,k_\perp^2) \tag{3}$$

In our analysis below we will not use the Sudakov decomposition, which is sometimes quite convenient in high-energy calculations. However, it is useful to have relations between our calculations and the results, where the Sudakov decomposition has been used. The corresponding analysis will be done in the next Section. Here we only note that the property $k^2 = -k_\perp^2$ (see Eq. (1)) comes from the fact that the Bjorken parton variable x in the standard and in the Sudakov approaches coincide.

Then, in the BFKL approach the SFs $F^c_{2,L}(x_B,Q^2)$ are driven at small x_B by gluons and are related in the following way to the unintegrated distribution $\varphi_g(x,k_\perp^2)$:

$$F^c_{2,L}(x_B,Q^2) \;=\; \int_{x_B}^1 \frac{dx}{x} \int \frac{dk_\perp^2}{k_\perp^2}\, C^g_{2,L}(x,Q^2,m_c^2,k_\perp^2)\; \varphi_g(x_B/x,k_\perp^2), \tag{4}$$

The functions $C^g_{2,L}(x,Q^2,m_c^2,k_\perp^2)$ may be regarded as the structure functions of the off-shell gluons with virtuality $k_\perp^2$ (hereafter we call them as *coefficient functions*). They are described by the quark box (and crossed box) diagram contribution to the photon-gluon interaction (see Fig. 1).

The purpose of the article is to calculate these coefficient functions $C^g_{2,L}(x,Q^2,m_c^2,k_\perp^2)$ and to analyze experimental data for $F_2^c(x_B,Q^2)$ by applying Eq. (4) with different sets of unintegrated gluon densities (see Ref. [14]) and to give predictions for the longitudinal SF $F_L^c(x_B,Q^2)$.

It is instructive to note that the diagrams shown in Fig. 1. are similar to those of the photon-photon scattering process. The corresponding QED contributions have been calculated many years ago in Ref. [15] (see also the beautiful review in Ref. [16]). Our results have been calculated independently and they are in full agreement with Ref. [15] (see Appendix B). However, we hope that our formulas which are given in a more simple form could be useful for others.

The structure of this article is as follows: in Sect. 2 we present the basic formalism of our approach with a brief review of the calculational steps (based on Ref. [17]). The connection of our analysis with the Sudakov-like approach is also given. Later, we present

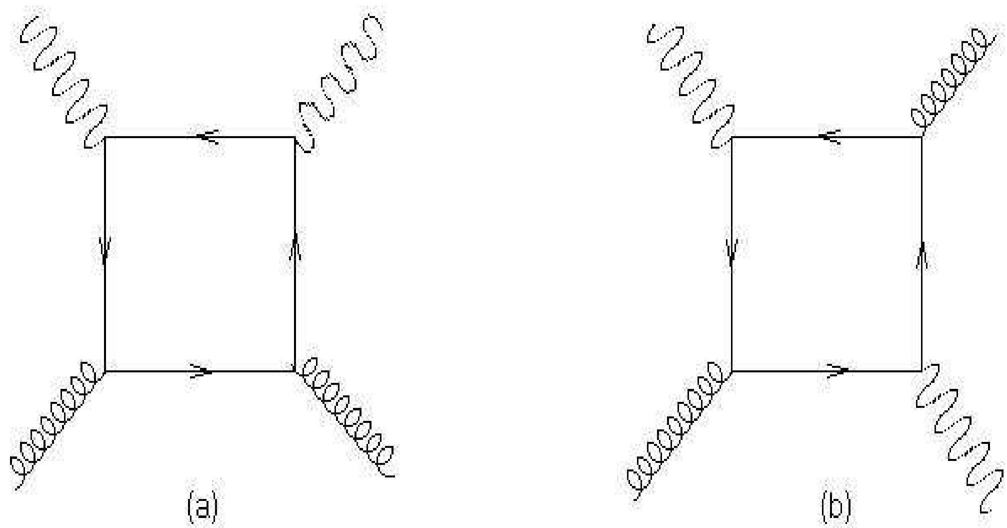

Figure 1: The diagrams contributing to $T_{\mu\nu}$ for a gluon target. They should be multiplied by a factor of 2 because of the opposite direction of the fermion loop. The diagram (a) should be also doubled because of crossing symmetry.

the results for the two most important polarization matrices for off-shell gluons into the proton. In Sect. 3 and 4 we give the predictions for the structure functions F_2^c and F_L^c for two cases of unintegrated gluon distribution functions (see Ref. [14]) used, which are shortly reviewed. In Appendix A we show the basic technique for the evaluation of the required Feynman diagrams. Appendix B contains the review of QED results from Refs. [15, 16]. In Appendix C we consider the limiting cases, when the values of the quark mass or the gluon momentum are equal to zero and also when the value of the photon "mass" Q^2 goes to zero.

2 Approach

The hadron part of the deep inelastic (DIS) spin-average lepton-hadron cross section can be represented in the form [1]:

$$F_{\mu\nu} \; = \; e_{\mu\nu}(q) \; F_L(x_B,Q^2) + d_{\mu\nu}(q,p) \; F_2(x_B,Q^2), \tag{5}$$

where q^μ and p^μ are the photon and hadron momenta,

$$e_{\mu\nu}(q) = g_{\mu\nu} - \frac{q_\mu q_\nu}{q^2} \quad \text{and} \quad d_{\mu\nu}(q,p) = -\left[g_{\mu\nu} + 2x_B \frac{(p_\mu q_\nu + p_\nu q_\mu)}{q^2} + p_\mu p_\nu \frac{4x_B^2}{q^2}\right]$$

and $F_k(x_B,Q^2)$ (hereafter $k = 2, L$) are structure functions.

The tensor $F_{\mu\nu}$ is connected via the optical theorem with the amplitude of elastic forward scattering of a photon on a hadron $T_{\mu\nu}(q,p)$, which may be decomposed in invariant amplitudes $T_k(x_B,Q^2)$ by analogy with Eq. (5).

Let us expand the invariant amplitudes in inverse powers of x_B:

$$T_k \; = \; \sum_{n=0}^{\infty} \left(\frac{1}{x_B}\right)^n T_{k,n} \tag{6}$$

The coefficients $T_{k,n}$ coincide (for even n) with the moments $M_{k,n}$ of the SF F_k:

$$T_{k,n} \; = \; M_{k,n} \equiv \int_0^1 dz \; z^{n-2} F_k(z,Q^2) \tag{7}$$

2.1 Evaluation of coefficient functions

We would like to note that the previous formalism can be replicated at parton level by replacing the hadron momentum p^μ by the gluon one k^μ and the Bjorken variable x_B by the corresponding x. Then, the hadron part of the deep inelastic spin-average lepton-parton cross section can be represented in the form

$$F^p_{\mu\nu} \; = \; e_{\mu\nu}(q) \; F^p_L(x,Q^2) + d_{\mu\nu}(q,k) \; F^p_2(x,Q^2), \tag{8}$$

where $F^p_k(x,Q^2)$ are the structure functions of lepton-parton DIS.

As in our analysis we only consider gluons, the unintegrated gluon distribution into the parton (i.e. into the gluon) $\varphi^p_g(x,k^2_\perp)$ should have the form

$$\varphi^g_g(x,k^2_\perp) \; = \; \delta(1-x)\hat{\varphi}(k^2_\perp),$$

[1] Hereafter we consider only one-photon exchange approximation.

where $\hat{\varphi}(k_\perp^2)$ is a function of $k_\perp^2$.

The parton SF $F_k^p(x,Q^2)$ and the amplitudes $T_k^p(x,Q^2)$ at the parton level obey equations similar to Eq. (6) and Eq. (7) with the replacement $x_B \to x$. Then, they are connected via optical theorem:

$$T_k^p(x,Q^2) \;=\; \sum_{n=0}^{\infty} \left(\frac{1}{x}\right)^n \int_0^1 dz\; z^{n-2} F_k^p(z,Q^2) \qquad (n=2m) \tag{9}$$

Thus, the coefficient functions $C_k^g(x,Q^2,k^2)$ of the parton SF $F_k^p(x,Q^2)$

$$F_{2,L}^p(x,Q^2) \;=\; \int \frac{dk_\perp^2}{k_\perp^2}\, C_{2,L}^g(y,Q^2,m_c^2,k_\perp^2)\Theta(x_0-x)\; \hat{\varphi}(k_\perp^2), \tag{10}$$

can be obtained directly using the amplitudes $T_k^p(x,Q^2)$ at the parton level

$$T_{2,L}^p(x,Q^2) \;=\; \int \frac{dk_\perp^2}{k_\perp^2}\, \tilde{C}_{2,L}^g(y,Q^2,m_c^2,k_\perp^2)\; \hat{\varphi}(k_\perp^2), \tag{11}$$

in the following way:

$$\tilde{C}_k^g(x,Q^2,k^2) \;=\; \sum_{n=0}^{\infty} \left(\frac{1}{x}\right)^n \int_0^1 dz\; z^{n-2} C_k^g(z,Q^2,k^2)\Theta(z_0-z), \tag{12}$$

where we have extracted a kinematical factor $\Theta(z_0-z)$.

As it was already discussed we will work with gluon part alone, keeping nonzero values of quark masses and the gluon virtuality. The corresponding Feynman diagrams are displayed on Fig. 1. The coefficient functions $C_k^g(x,Q^2,k^2)$ do not depend on the target type. So, it can be calculated in photon-parton DIS and used later in the photon-hadron reaction (see Eq. (4)).

2.2 Connection with the Sudakov-like approach

One of the basic ingredients in the Sudakov-like approach is the introduction of an additional light-cone momentum n^μ with $n^2=0$ and $(np)=1$.

The gluon momentum k^μ can be represented as

$$k^\mu = \xi p^\mu + \frac{k^2+k_\perp^2}{2\xi} n^\mu + k_T^\mu \tag{13}$$

with the following properties

$$p^2 = n^2 = (pk_T) = (nk_T) = 0, \quad (np) = 1 \tag{14}$$

where the four-vector k_T^μ contains only the transverse part of k^μ, $k_T = (0, k_\perp, 0)$, i.e. $k_T^2 = -k_\perp^2$. and $\xi = x_B/x$ is the fraction of the proton momentum carried by the gluon (see Eq. (4).

To study the relations between the "usual" approach used here and the Sudakov-like one, it is convenient to introduce the following parametrization for the vector n^μ (see Ref. [18])

$$n^\mu = \frac{2x_B}{Q^2}\left(x_B p^\mu + q^\mu\right) \tag{15}$$

It is easy to check that the properties in Eq. (14) are fulfilled.

Then, for the scalar product (kq) we have in the Sudakov-like approach:

$$\begin{aligned}(kq) &= \xi\,(pq) + \frac{k^2 + k_\perp^2}{2\xi}\,(nq) \\ &= \frac{Q^2}{2x}\left[1 - x^2\frac{k^2 + k_\perp^2}{Q^2}\right]\end{aligned} \tag{16}$$

If $k^2 = -k_\perp^2$, then it follows from Eq. (16)

$$x = \frac{Q^2}{2(kq)},$$

that agrees with Eq. (2). Also from Eq. (13) it follows

$$k^\mu = xp^\mu + k_T^\mu, \tag{17}$$

where x is the fraction of the proton momentum carried by the gluon.

2.3 Feynman-gauge gluon polarization

As a first approximation we consider gluons having polarization tensor (hereafter the indices α and β are connected with gluons and μ and ν are connected with photons)[2]:

$$\hat{P}^{\alpha\beta} = -g^{\alpha\beta} \tag{18}$$

This polarization tensor corresponds to the case when gluons do not interact. In some sense the case of polarization is equal to the standard DIS suggestions about parton

[2]In principle, we can use here more general cases of polarization tensor (for example, that one based on the Landau or unitary gauge). The difference between them and Eq. (18) is $\sim k^\alpha$ and/or $\sim k^\beta$ and, hence, it leads to zero contributions because the Feynman diagrams in Fig.1 are gauge invariant.

properties, excepting their off-shell property. The polarization in Eq. (18) gives the main contribution to the polarization tensor we are interested in (see below)

$$\hat{P}^{\alpha\beta}_{BFKL} = \frac{k_\perp^\alpha k_\perp^\beta}{k_\perp^2} = \frac{x^2}{-k^2} p^\alpha p^\beta, \tag{19}$$

which comes from the high energy (or k_T) factorization prescription [19, 20, 21] [3].

Contracting the photon projectors (connected with photon indices of diagrams in Fig.1.)

$$\hat{P}^{(1)}_{\mu\nu} = -\frac{1}{2} g_{\mu\nu} \quad \text{and} \quad \hat{P}^{(2)}_{\mu\nu} = 4x^2 \frac{k_\mu k_\nu}{Q^2}$$

with the hadronic tensor $F_{\mu\nu}$, we obtain the following relations at the parton level (i.e. for off-shell gluons having momentum k_μ)

$$\tilde{\beta}^2 \, C^g_2(x) \;=\; \mathcal{K} \, \left[f^{(1)} + \frac{3}{2\tilde{\beta}^2} \, f^{(2)} \right] \tag{20}$$

$$\tilde{\beta}^2 \, C^g_L(x) \;=\; \mathcal{K} \, \left[4bx^2 f^{(1)} + \frac{(1+2bx^2)}{\tilde{\beta}^2} \, f^{(2)} \right] \;=\; \mathcal{K} \, f^{(2)} + 4bx^2 \tilde{\beta}^2 \, C^g_2, \tag{21}$$

where the normalization factor $\mathcal{K} = e_c^2 \, \alpha_s(Q^2)/(4\pi) \, x$,

$$P^{(i)}_{\mu\nu} F_{\mu\nu} = \mathcal{K} \, f^{(i)}, \; i = 1, 2$$

and $\tilde{\beta}^2 = 1 - 4bx^2, \quad b = -k^2/Q^2 \equiv k_\perp^2/Q^2 > 0, \quad a = m^2/Q^2$. The kinematical factor z_0 which appear in Eq. (12) is

$$z_0 \;=\; \frac{1}{1+4a+b} \tag{22}$$

Applying the projectors $\hat{P}^{(i)}_{\mu\nu}$ to the Feynman diagrams displayed in Fig.1, we obtain [4] the following results for the contributions to expressions

$$\begin{aligned} f^{(1)} \;&=\; -2\beta \Big[1 - \Big(1 - 2x(1+b-2a) \, [1 - x(1+b+2a)] \Big) \, f_1 \\ &+\; (2a-b)(1-2a)x^2 \; f_2 \Big], \end{aligned} \tag{23}$$

$$\begin{aligned} f^{(2)} \;&=\; 8x \, \beta \Big[(1-(1+b)x) - 2x \Big(bx(1-(1+b)x)(1+b-2a) + a\tilde{\beta}^2 \Big) \, f_1 \\ &+\; bx^2(1-(1+b)x)(2a-b) \; f_2 \Big], \end{aligned} \tag{24}$$

---

[3] We would like to note that the BFKL polarization tensor is a particular case of so-called nonsense polarization of the particles in t-channel makes the main contributions for cross sections in s-channel at $s \to \infty$ (see, for example, Ref. [22] and references therein). The limit $s \to \infty$ corresponds to the small values of Bjorken variable x_B, that is just the range of our study.

[4] The contributions of individual scalar components of the diagrams of Fig.1 (which come after evaluation of traces of γ-matrices) are given in Appendix A.

where

$$\beta^2 = 1 - \frac{4ax}{(1-(1+b)x)}$$

and [5]

$$f_1 = \frac{1}{\tilde{\beta}\beta}\, ln\frac{1+\beta\tilde{\beta}}{1-\beta\tilde{\beta}}, \qquad f_2 = \frac{-4}{1-\beta^2\tilde{\beta}^2}$$

The important regimes: $k^2 = 0$, $m^2 = 0$ and $Q^2 \to 0$ are considered in Appendix C. The $Q^2 = 0$ limit is given in Sect. 2.5.

2.4 BFKL-like gluon polarization

Now we take into account the BFKL gluon polarization given in Eq. (19). As we already noted in previous subsection, in these calculations we did not use Sudakov decomposition and, hence, the hadron momentum p^α is not so convenient variable in our case. Thus, we represent the projector $\hat{P}^{\alpha\beta}_{BFKL}$ as a combination of projectors constructed by the momenta k^α and q^α.

We can represent the tensor $F^{\alpha\beta}$ in the general form:

$$F^{\alpha\beta} \;=\; Ag^{\alpha\beta} + Bq^\alpha q^\beta + Ck^\alpha k^\beta + D\left(k^\alpha q^\beta + q^\alpha k^\beta\right), \tag{25}$$

where A, B, C and D are some scalar functions of the variables y, a and b.

¿From the gauge invariance of the vector current: $k^\alpha F^{\alpha\beta} = k^\beta F^{\alpha\beta} = 0$ we have the following relations

$$C\; k^2 \;=\; -\left[A + D\;(kq)\right], \quad B\;(kq) \;=\; -\,D\;k^2 \tag{26}$$

If we apply the BFKL-like projector $\hat{P}^{\alpha\beta}_{BFKL}$ and use the light-cone properties given in Eq. (14), we get the simple relation

$$\hat{P}^{\alpha\beta}_{BFKL}F^{\alpha\beta} \;=\; D\;(kq) \tag{27}$$

The standard projectors $g^{\alpha\beta}$ and $q^\alpha q^\beta$ lead to the relations

$$g^{\alpha\beta}F^{\alpha\beta} \;=\; 3A + D\frac{Q^2}{2x}\tilde{\beta}^2 \tag{28}$$

$$q^\alpha q^\beta F^{\alpha\beta} \;=\; \frac{\tilde{\beta}^2}{bx^2}\left[3A + D\frac{Q^2}{2x}\tilde{\beta}^2\right] \tag{29}$$

[5] We use the variables as defined in Ref. [23].

¿From Eqs. (26), (28) and (29) we have

$$\left[\left((kq)^2 - k^2q^2\right) g^{\alpha\beta} + 3k^2 q^\alpha q^\beta\right] F^{\alpha\beta} \;=\; -\, D\frac{Q^8}{4x^4}\tilde{\beta}^4 \tag{30}$$

and the BFKL-like projector $\hat{P}^{\alpha\beta}_{BFKL}$ can be represented as

$$\hat{P}^{\alpha\beta}_{BFKL} \;=\; -\frac{1}{2}\frac{1}{\tilde{\beta}^4}\left[\tilde{\beta}^2 g^{\alpha\beta} - 12bx^2\frac{q^\alpha q^\beta}{Q^2}\right] \tag{31}$$

In the previous section we have already calculated the contributions to coefficient functions using the first term within the brackets in the r.h.s. of Eq. (31). Repeating the above calculations with the projector $\sim q^\alpha q^\beta$, we obtain the total contribution to the coefficient functions which can be represented as the following shift in the results given in Eqs. (20)- (24):

$$\begin{aligned}
C^g_2(x) \;&\to\; C^g_{2,BFKL}(x), \quad C^g_L(x) \;\to\; C^g_{L,BFKL}(x); \\
f^{(1)} \;&\to\; f^{(1)}_{BFKL} = \frac{1}{\tilde{\beta}^4}\left[\tilde{\beta}^2 f^{(1)} \;-\; 3bx^2\tilde{f}^{(1)}\right] \\
f^{(2)} \;&\to\; f^{(2)}_{BFKL} = \frac{1}{\tilde{\beta}^4}\left[\tilde{\beta}^2 f^{(2)} \;-\; 3bx^2\tilde{f}^{(2)}\right],
\end{aligned} \tag{32}$$

where

$$\begin{aligned}
\tilde{f}^{(1)} \;&=\; -\beta\left[\frac{1-x(1+b)}{x} - 2\Big(x(1-x(1+b))(1+b-2a) + a\tilde{\beta}^2\Big)\, f_1\right. \\
&\left.-\;\; x(1-x(1+b))(1-2a)\; f_2\right],
\end{aligned} \tag{33}$$

$$\tilde{f}^{(2)} \;=\; 4\,\beta\,(1-(1+b)x)^2\left[2-(1+2bx^2)\, f_1 - bx^2\; f_2\right], \tag{34}$$

For the important regimes when $k^2 = 0$, $m^2 = 0$ and $Q^2 \to 0$, the analyses are given in Appendix C.

Notice that our results in Eqs. (33) and (34) should coincide with the integral representations of Refs. [19, 25] (at $Q^2 \to 0$ there is full agreement (see following subsection) with the formulae of Refs. [19, 25] for photoproduction of heavy quarks). Our results in Eqs. (33) and (34) should also agree with those in Ref. [24] but the direct comparison is quite difficult because the authors of Ref. [24] used a different (and quite complicated) way to obtain their results and the structure of their results is quite cumbersome (see Appendix A in Ref. [24]). We have found numerical agreement in the case of $F_2(x_B, Q^2)$ (see Sect. 3 and Fig.4).

2.5 $Q^2 = 0$ limit and Catani-Ciafaloni-Hautmann approach

We introduce the new variables $\hat{s}$, ρ and Δ which are useful in the limit $Q^2 \to 0$:

$$\hat{s} = \frac{Q^2}{x}, \quad \rho = 4ax \equiv \frac{4m^2}{\hat{s}}, \quad \Delta = bx \equiv \frac{-k^2}{Q^2}x = \frac{k_\perp^2}{\hat{s}} \tag{35}$$

and express our formulae above as functions of ρ and Δ at small x asymptotic (i.e. small Q^2).

When $x = 0$ we have got the following relations:
for the intermediate functions

$$\tilde{\beta}^2 = 1, \quad \beta^2 = 1 - \frac{\rho}{1-\Delta} \equiv \hat{\beta}^2, \quad f_1 = \frac{1}{\hat{\beta}} ln \frac{1+\hat{\beta}}{1-\hat{\beta}} \equiv L(\hat{\beta}), \quad f_2 = \frac{4\hat{\beta}}{\rho}(1-\Delta) \tag{36}$$

$$\begin{aligned} f^{(1)} &= 2\hat{\beta}\Bigg[\left(1+\rho-\frac{\rho^2}{2}\right)L(\hat{\beta}) - (1-\rho) + \left(2+\rho-2L(\hat{\beta})\right)\Delta \\ &+ 2\left(L(\hat{\beta})-1\right)\Delta^2\Bigg], \end{aligned} \tag{37}$$

$$x\tilde{f}^{(1)} = -2\hat{\beta}\Big[2(1-\Delta) - \rho L(\hat{\beta})\Big], \quad f^{(2)} = x\tilde{f}^{(2)} = 0, \tag{38}$$

and, thus, for the coefficient functions

$$C_L^g = 0, \qquad C_2^g = \mathcal{K}\, f_{BFKL}^{(1)}, \tag{39}$$

where

$$\begin{aligned} f_{BFKL}^{(1)} &= 2\hat{\beta}\Bigg[\left(1+\rho-\frac{\rho^2}{2}\right)L(\hat{\beta}) - (1+\rho) + \left(8+\rho-(2+3\rho)L(\hat{\beta})\right)\Delta \\ &+ 2\left(L(\hat{\beta})-4\right)\Delta^2\Bigg], \end{aligned} \tag{40}$$

We note that the results coincide exactly with those from Catani-Ciafaloni-Hautmann work in Ref. [19, 25] (see Eq. (2.2) in Ref. [25]) in the case of photoproduction of heavy quarks. The $O(x)$ contribution in the $Q^2 \to 0$ limit is given in Appendix C (see subsection C.3).

3 Comparison with F_2^c experimental data

With the help of the results obtained in the previous Section we have analyzed HERA data for SF F_2^c from ZEUS [3] and H1 [4] collaborations.

3.1 Unintegrated gluon distribution

In this paper we consider two different parametrizations for the unintegrated gluon distribution [14]. Firstly, we use the parametrization based on the numerical solution of the BFKL evolution equation [26] (RS–parametrization). The solution has the following form [26]:

$$\begin{aligned}\Phi(x,k^2) &= \frac{a_1}{a_2+a_3+a_4}\left[a_2+a_3\,\frac{Q_0^2}{k^2}+\left(\frac{Q_0^2}{k^2}\right)^2+\alpha\,x+\frac{\beta}{\epsilon+\ln(1/x)}\right] \\ & C_q\left[\frac{a_5}{a_5+x}\right]^{1/2}\Big[1-a_6x^{a_7}\ln\left(k^2/a_8\right)\Big]\,(1+a_{11}x)(1-x)^{a_9+a_{10}\ln(k^2/a_8)}, \quad (41)\end{aligned}$$

where

$$C_q = \begin{cases} 1, & \text{if} \quad k^2 < q_0^2(x), \\ q_0^2(x)/k^2, & \text{if} \quad k^2 > q_0^2(x) \end{cases} \qquad (42)$$

The parameters ($a_1 - a_{11}, \alpha, \beta$ and ϵ) were found (see Ref. [26]) by minimization of the differences between the l.h.s and the r.h.s. of the BFKL-type equation for the unintegrated gluon distribution $\Phi(x,k^2)$ with 'Q_0^2 =4 GeV^2.

Secondly, we also use the results of a BFKL-like parametrization of the unintegrated gluon distribution $\Phi(x,k_\perp^2,\mu^2)$, according to the prescription given in Ref. [27]. The proposed method lies upon a straightforward perturbative solution of the BFKL equation where the collinear gluon density $x\,G(x,\mu^2)$ from the standard GRV set [28] is used as the boundary condition in the integral form of Eq. (1). Technically, the unintegrated gluon density is calculated as a convolution of the collinear gluon density $G(x,\mu^2)$ with universal weight factors [27]:

$$\Phi(x,k_\perp^2,\mu^2) = \int_x^1 \mathcal{G}(\eta,k_\perp^2,\mu^2)\,\frac{x}{\eta}\,G(\frac{x}{\eta},\mu^2)\,d\eta, \qquad (43)$$

where

$$\mathcal{G}(\eta,k_\perp^2,\mu^2) = \frac{\bar{\alpha}_s}{\eta k_\perp}\begin{cases} J_0(2\sqrt{\bar{\alpha}_s\ln(1/\eta)\ln(\mu^2/k_\perp^2)}), & \text{if} \quad k_\perp^2 < \mu^2, \\ I_0(2\sqrt{\bar{\alpha}_s\ln(1/\eta)\ln(k_\perp^2/\mu^2)}), & \text{if} \quad k_\perp^2 > \mu^2 \end{cases}, \qquad (44)$$

20xun01 where J_0 and I_0 stand for Bessel functions (of real and imaginary arguments, respectively), and $\bar{\alpha}_s = 3\alpha_s/\pi$. The parameter $\bar{\alpha}_s$ is connected with the Pomeron trajectory intercept: $\Delta_P = \bar{\alpha}_s 4 \ln 2$ in the LO and $\Delta_P = \bar{\alpha}_s 4 \ln 2 - N\bar{\alpha}_s^2$ in the NLO approximations, where N is a number, $N \sim 18$ [29]-[31]. However, some resummation procedures proposed in the last years lead to positive value of $\Delta_P \sim 0.2 - 0.3$ (see Refs. [32, 33] and references therein).

Therefore, in our calculations with Eq. (43) we only used the solution of the LO BFKL equation and considered Δ_P as a free parameter varying it from 0.166 to 0.53. This approach was used for the description of the p_T spectrum of D^* meson electroproduction at HERA [34] where the value for the Pomeron intercept parameter $\Delta_P = 0.35$ was obtained [6]. We used this value of Δ_P in our present calculations with $\mu^2 = Q_0^2 = 1 - 4$ GeV^2.

3.2 Numerical results

For the calculation of the SF F_2^c we use Eq. (4) in the following form:

$$\begin{aligned} F_2^c(x, Q^2) &= \int_{x(1+4a)}^1 \frac{dy}{y} C_2^g(\frac{x}{y}, Q^2, 0)\, yG(y, Q_0^2) + \\ &+ \sum_{i=1}^2 \int_{y_{min}^{(i)}}^{y_{max}^{(i)}} \frac{dy}{y} \int_{k_{\perp min}^{2(i)}}^{k_{\perp max}^{2(i)}} dk_\perp^2\, C_2^g(\frac{x}{y}, Q^2, k_\perp^2)\, \Phi(y, k_\perp^2, Q_0^2). \end{aligned} \tag{45}$$

Here $\Phi(y, k_\perp^2, Q_0^2) = \frac{1}{k_\perp^2}\varphi_g(y, k_\perp^2, Q_0^2)$ and the changes $x_B \to x, x \to y$ were done in comparison with Eq. (4). The coefficient function $C_2^g(x)$ is given in Eq. (20) with $f_{BFKL}^{(1)}$ and $f_{BFKL}^{(2)}$ instead of $f^{(1)}$ and $f^{(2)}$, respectively (see Eq. (32)). The functions $f^{(1)}$ and $f^{(2)}$ in Eq. (20) are given by Eqs. (23) and (24), respectively, and the functions $\tilde{f}^{(1)}$ and $\tilde{f}^{(2)}$ can be found in Eqs. (33) and (34), respectively.

The integration limits in Eq. (45) have the following values:

$$\begin{aligned} y_{min}^{(1)} &= x(1 + 4a + \frac{Q_0^2}{Q^2}), \quad y_{max}^{(1)} = 2x(1+2a); \\ k_{\perp min}^{2(1)} &= Q_0^2, \quad k_{\perp max}^{2(1)} = (\frac{y}{x} - (1+4a))Q^2; \\ y_{min}^{(2)} &= 2x(1+2a), \quad y_{max}^{(2)} = 1; \\ k_{\perp min}^{2(2)} &= Q_0^2, \quad k_{\perp max}^{2(2)} = Q^2; \end{aligned} \tag{46}$$

[6] Close values for the parameter Δ_P were obtained, rather, in very different papers (see, for example, Ref. [35]) and in the L3 experiment [36].

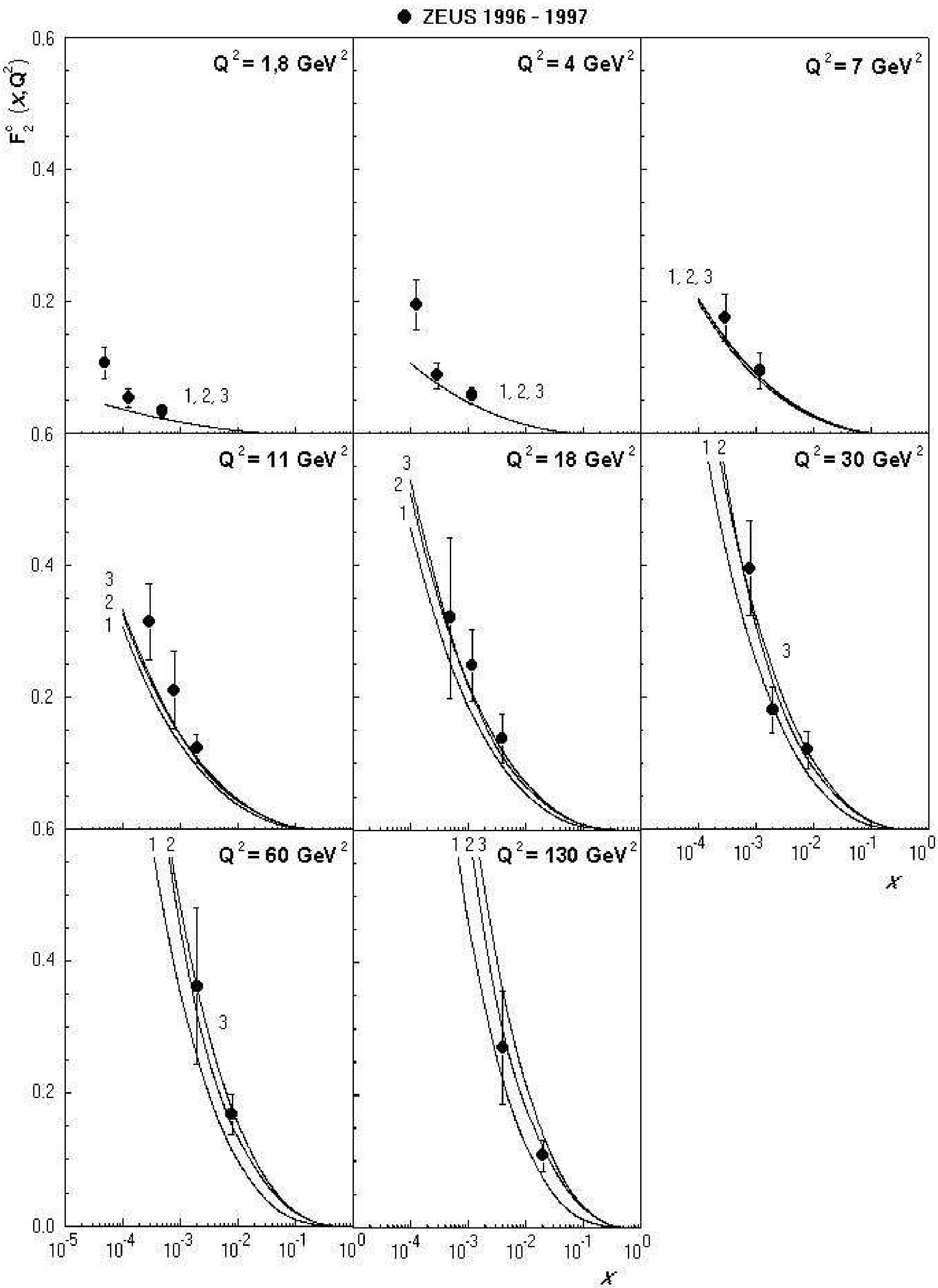

Figure 2: The structure function $F_2^c(x, Q^2)$ as a function of x for different values of Q^2 compared to ZEUS data [3]. Curves 1, 2 and 3 correspond to SF obtained in the standard parton model with the GRV [28] gluon density at the leading order approximation and to SF obtained in the k_T factorization approach with RS [26] and BFKL (at $Q_0^2 = 4$ GeV^2) [27] parametrizations of unintegrated gluon distribution.

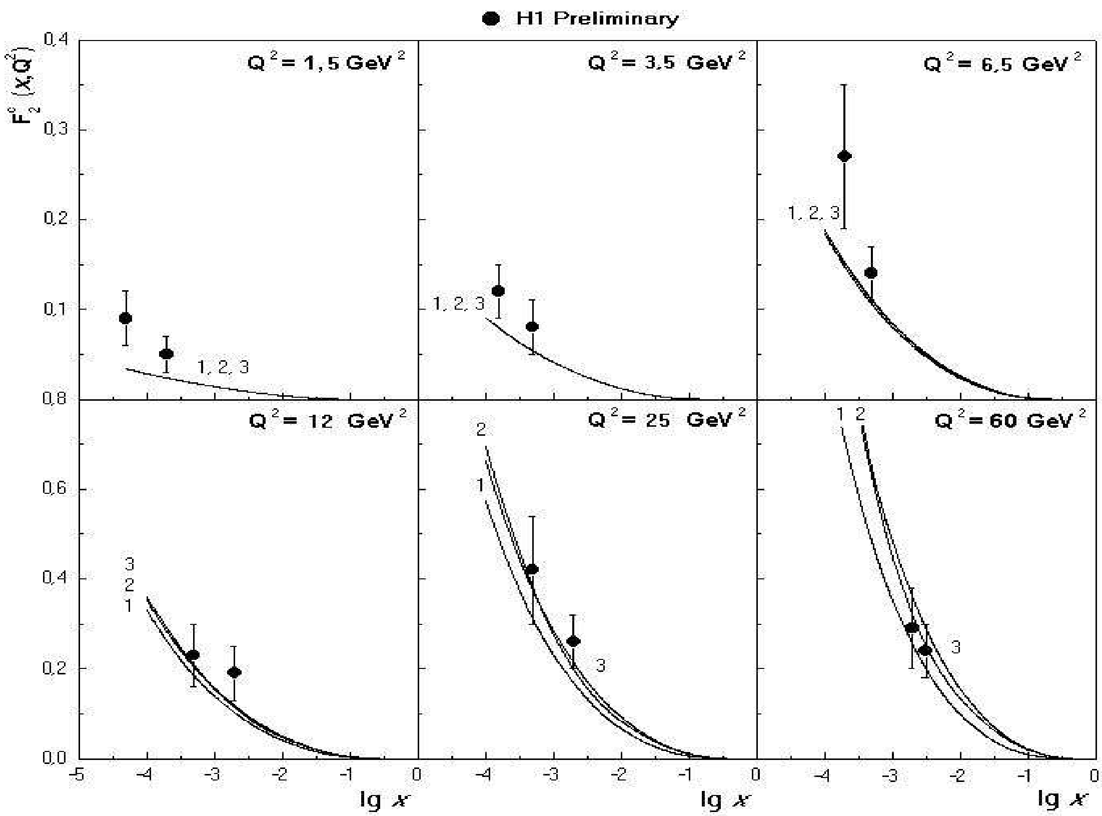

Figure 3: The structure function $F_2^c(x,Q^2)$ as a function of x for different values of Q^2 compared to H1 data [4]. Curves 1, 2 and 3 are as in Fig. 2.

The ranges of integration correspond to the requirement of positive values in the arguments of the square roots in Eqs. (23), (24), (33) and (34) and also obey to the kinematical restriction $(z \equiv x/y) \leq z_0$ with z_0 from Eq. (22).

In Figs. 2 and 3 we show the SF F_2^c as a function x for different values of Q^2 in comparison with ZEUS [3] and H1 [4] experimental data. For comparison we present the results of the calculation with two different parametrizations for the unintegrated gluon distribution $\Phi(x, k_\perp^2, Q_0^2)$ in the forms given by Eq. (41) and Eq. (43) at $Q_0^2 = 4$ GeV^2.

The differences observed between the curves 2 and 3 are due to the different behaviour of the unintegrated gluon distribution as function x and $k_\perp$.

We see that at large Q^2 ($Q^2 \geq 10$ GeV^2) the SF F_2^c obtained in the k_T factorization approach is higher than the SF obtained in the standard parton model with the GRV

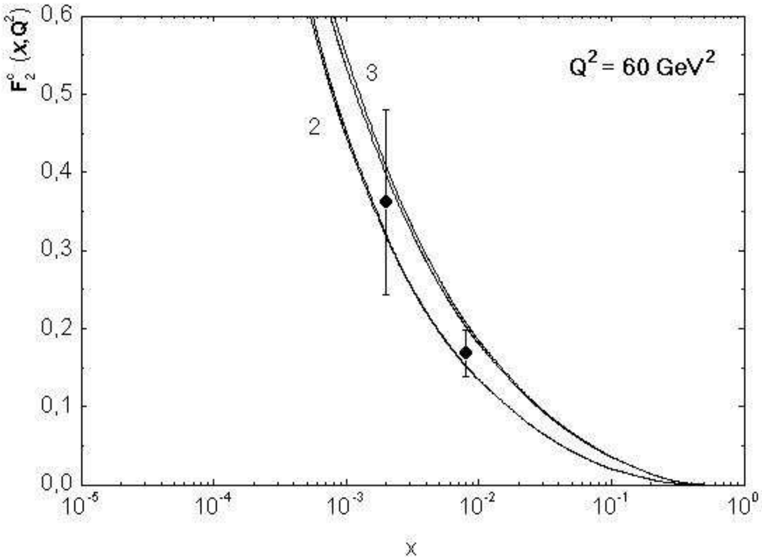

Figure 4: The structure function $F_2^c(x, Q^2)$ as a function of x at $Q^2 = 60$ GeV^2 compared to ZEUS data [3]. Curves 2 and 3 correspond to RS (at $Q_0^2 = 4$ GeV^2) [26] and BFKL (at $Q_0^2 = 1$ GeV^2) [27] parametrizations obtained with our off mass shell matrix and ones from Ref. [24].

gluon density at the LO approximation (see curve 1) and has a more rapid growth in comparison with the standard parton model results, especially at $Q^2 \sim 130$ GeV^2 [37]. At $Q^2 \leq 10$ GeV^2 the predictions from perturbative QCD (in GRV approach) and those based on the k_T factorization approach are very similar [7] and show the disagreement with data below $Q^2 = 7$ GeV^2 [8]. Unfortunately the available experimental data do not permit yet to distinguish the k_T factorization effects from those due to boundary conditions [26].

Fig. 4 shows the structure function F_2^c at $Q^2 = 60$ GeV^2 obtained with two different gluon densities, i.e. RS (at $Q_0^2 = 4$ GeV^2) and BFKL (at $Q_0^2 = 1$ GeV^2) parametrizations. The difference between curves 2 and 3 are mainly due to the different Q_0^2 value used (as we have already shown in Figs. 2 and 3, the difference due to the parametrizations is

[7] This fact is due to the quite large value of $Q_0^2 = 4$ GeV^2 chosen here.

[8] A similar disagreement with data at $Q^2 \leq 2$ GeV^2 has been observed for the complete structure function F_2 (see, for example, the discussion in Ref. [38] and reference therein). We note that the insertion of higher-twist corrections in the framework of usual perturbative QCD improves the agreement with data (see Ref. [39]) at quite low values of Q^2.

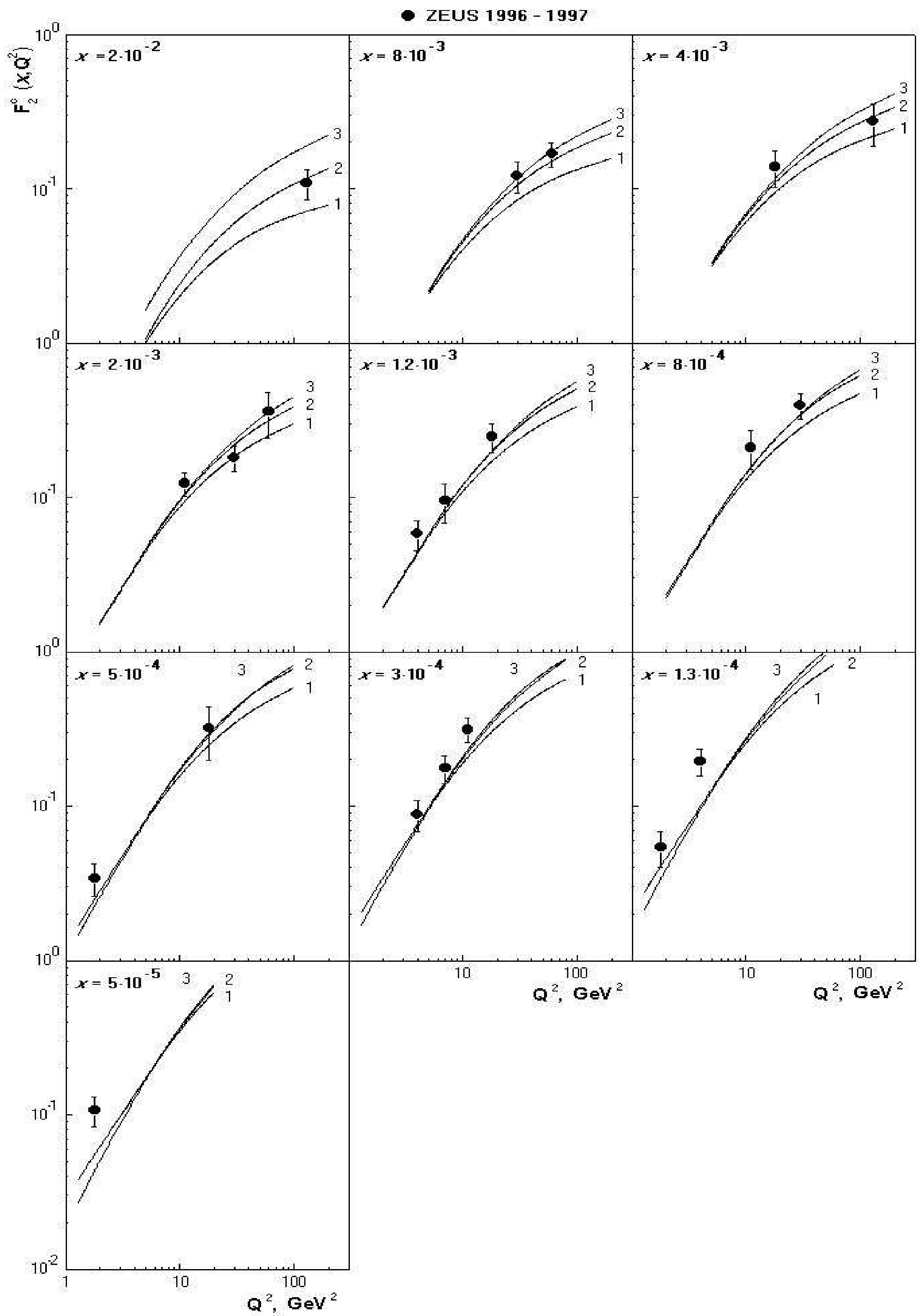

Figure 5: The structure function $F_2^c(x, Q^2)$ as a function of Q^2 for different values of x compared to ZEUS data [3]. Curves 1, 2 and 3 are as in Fig. 2.

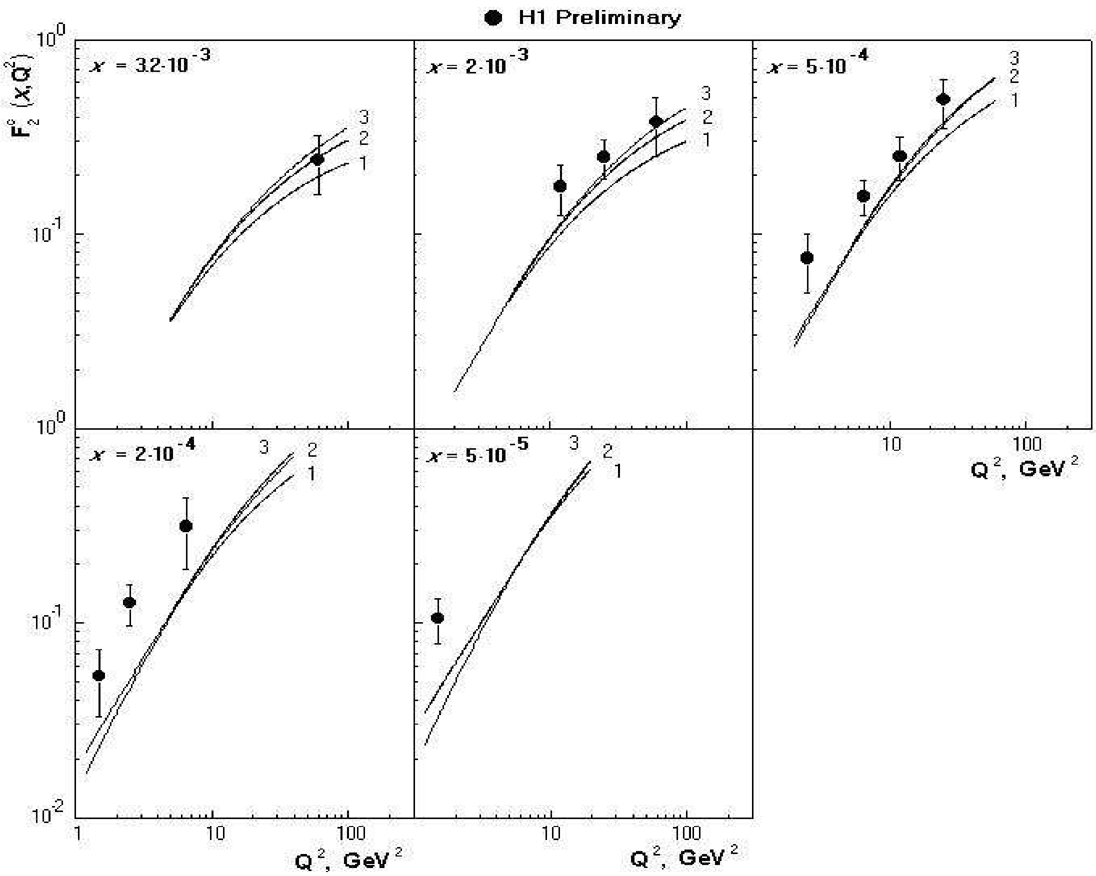

Figure 6: The structure function $F_2^c(x, Q^2)$ as a function of Q^2 for different values of x compared to H1 data [4]. Curves 1, 2 and 3 are as in Fig. 2.

essentially smaller). From Figs. 2, 3 and 4, we note that the difference between the k_T factorization results and those from perturbative QCD increases when we change the value of Q_0^2 in Eq. (3) from 4 GeV^2 to 1 GeV^2 [37]. In addition, for each case presented in Fig. 4. we have done the calculations with our off mass shell matrix elements and those from Ref. [24] [9]. The predictions are very similar and cannot be distinguished on curves 2 and 3.

For completeness, in Figs. 5 and 6 we present the SF F_2^c as a function Q^2 for different values of x in comparison with ZEUS [3] and H1 [4] experimental data.

[9] We would like to note that Ref. [24] contains several slips: the propagators in Eq. (A.1) and the products (pq) in Eqs. (A.4) and (A.5) should be in the denominator, the indices 2 and L in Eqs. (A.4) and (A.5) should be transposed.

4 Predictions for F_L^c

To calculate the SF F_L^c we have used Eq. (45) with the replacement of the coefficient function C_2^g by C_L^g, which is given by Eq. (21).

In Fig. 7 we show the predictions for F_L^c obtained with different unintegrated gluon distributions. The difference between the results obtained in perturbative QCD and from the k_T factorization approach is quite similar to the F_2^c case discussed above.

The ratio $R^c = F_L^c/F_2^c$ is shown in Fig. 8. We see $R^c \approx 0.1 \div 0.3$ in a wide region of Q^2. The estimation of R^c is very close to the results for $R = F_L/(F_2 - F_L)$ ratio (see Refs. [40]-[43]). We would like to note that these values of R^c contradict the estimation obtained in Refs. [3, 4]. The effect of R^c on the corresponding differential cross-section should be considered in the extraction of F_2^c from future more precise measurements.

For the ratio R^c we found quite flat x-behavior at low x in the low Q^2 region (see Fig. 8), where approaches based on perturbative QCD and on k_T factorization give similar predictions (see Fig 2, 3, 5, 6 and 7). It is in agreement with the corresponding behaviour of the ratio $R = F_L/(F_2 - F_L)$ (see Ref. [40]) at quite large values of Δ_P [10] ($\Delta_P > 0.2 - 0.3$). The low x rise of R^c at high Q^2 disagrees with early calculations [40] in the framework of perturbative QCD. It could be due to the small x resummation, which is important at high Q^2 (see Fig 2, 3, 5, 6 and 7). We plan to study in future this effect on R in the framework of k_T factorization.

5 Conclusions

We have performed the calculation of the perturbative parts for the structure functions F_2^c and F_L^c for a gluon target having nonzero momentum squared, in the process of photon-gluon fusion. The results have quite compact form for both: the Feynman gauge and a nonsense (or BFKL-like) gluon polarizations.

We have applied the results in the framework of k_T factorization approach to the analysis of present data for the charm contribution to F_2 (F_2^c) and we have given the

[10] At small values of Δ_P, i.e. when $x^{-\Delta_P} \sim Const$, the ratio R tends to zero at $x \to 0$ (see Ref. [44]).

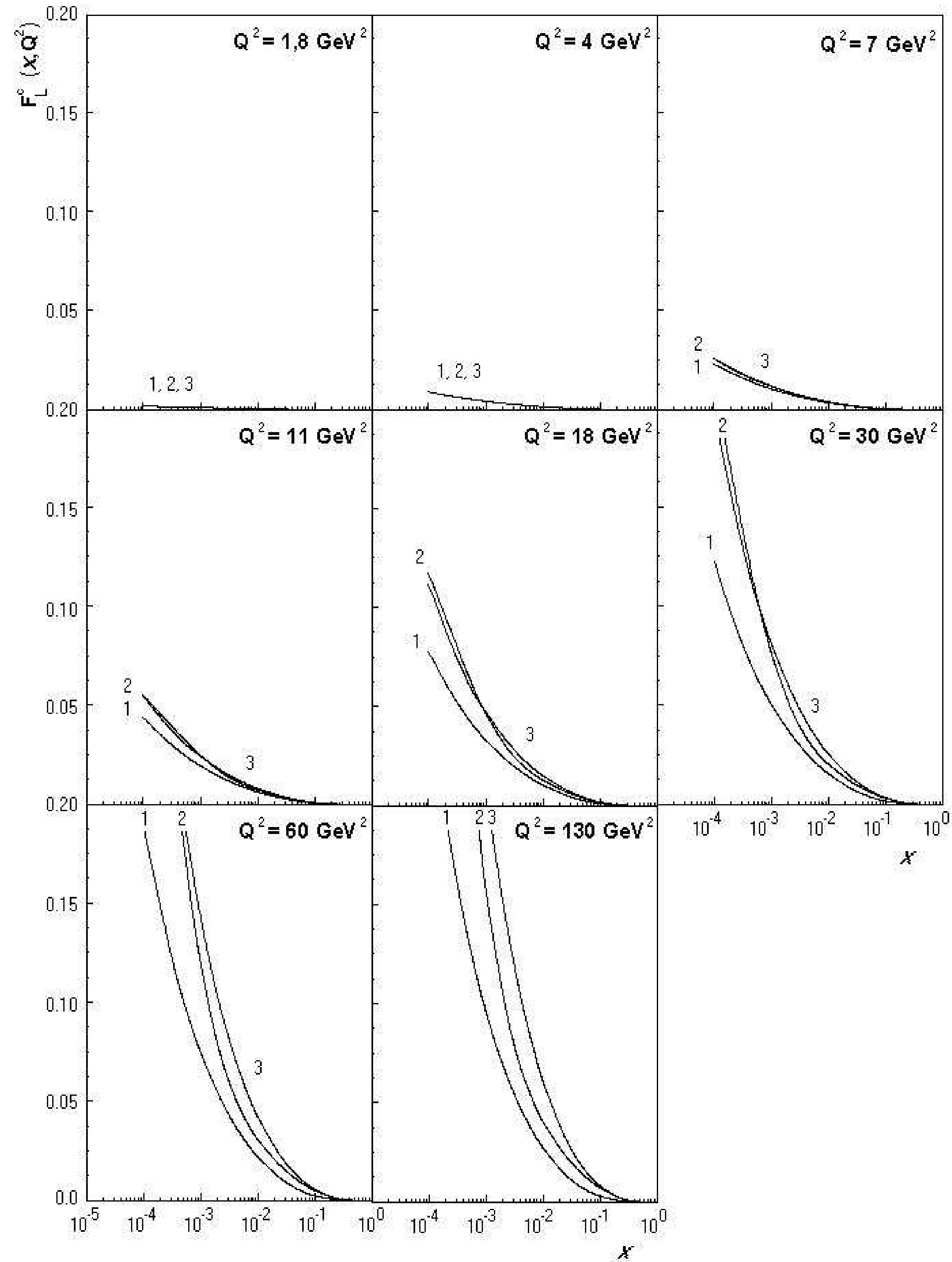

Figure 7: The structure function $F_L^c(x, Q^2)$ as a function of x for different values of Q^2. Curves 1, 2 and 3 are as in Fig. 2.

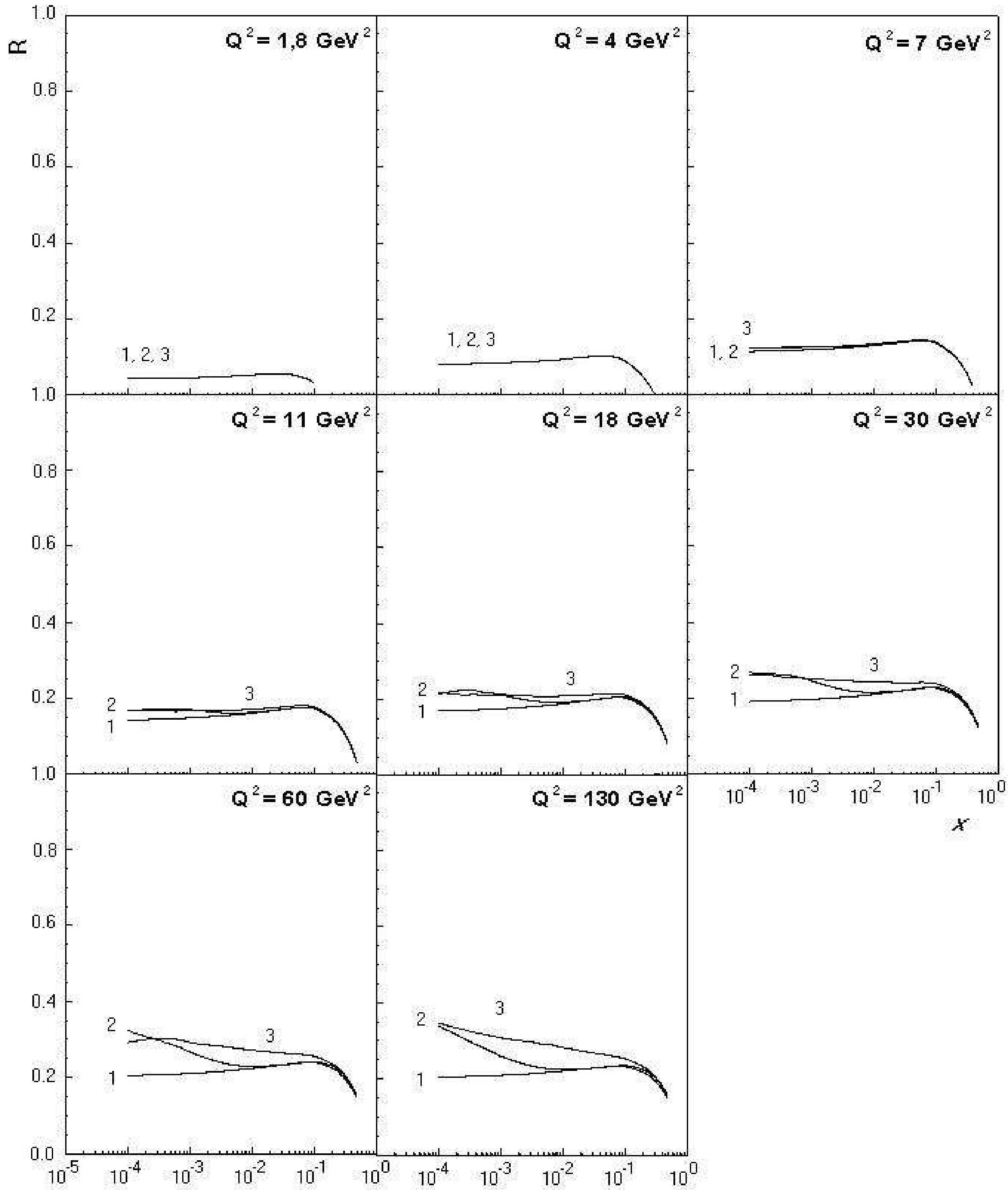

Figure 8: The ratio $R^c = F_L^c(x, Q^2)/F_2^c$ as a function of x for different values of Q^2. Curves 1, 2 and 3 are as in Fig. 2.

predictions for F_L^c. The analysis has been performed with several parametrizations of unintegrated gluon distributions (RS and BFKL) for comparison. We have found good agreement of our results, obtained with RS and BFKL parametrizations of unintegrated gluons distributions at $Q_0^2 = 4$ GeV^2, with experimental F_2^c HERA data, except at low Q^2 ($Q^2 \leq 7$ GeV^2) [11]. We have also obtained quite large contribution of the SF F_L^c at low x and high Q^2 ($Q^2 \geq 30$ GeV^2).

We would like to note the good agreement between our results for F_2^c and the ones obtained in Ref. [45] by Monte-Carlo studies. Moreover, we have also good agreement with fits of H1 and ZEUS data for F_2^c (see recent reviews in Ref. [46] and references therein) based on perturbative QCD calculations at NLO. But unlike to these fits, our analysis uses universal unintegrated gluon distribution, which gives in the simplest way the main contribution to the cross-section in the high-energy limit.

It could be also very useful to evaluate the complete F_2 itself and the derivatives of F_2 with respect to the logarithms of $1/x$ and Q^2 with our expressions using the unintegrated gluons. We are considering to present this work and also the predictions for F_L in a forthcoming article.

The consideration of the SF F_2 in the framework of the leading-twist approximation of perturbative QCD (i.e. for "pure" perturbative QCD) leads to very good agreement (see Ref. [38] and references therein) with HERA data at low x and $Q^2 \geq 1.5$ GeV^2. The agreement improves at lower Q^2 when higher twist terms are taken into account [39]. As it has been studied in Refs. [38, 39], the SF F_2 at low Q^2 is sensitive to the small-x behavior of quark distributions. Thus, the analysis of F_2 in a broader Q^2 range should require the incorporation of parametrizations for unintegrated quark densities, introduced recently (see Ref. [47] and references therein).

The study of the complete SF F_L should also be very interesting. The structure function F_L depends strongly on the gluon distribution (see, for example, Ref. [48]), which in turn is determined [49] by the derivative $dF_2/dlnQ^2$. Thus, in the framework of perturbative QCD at low x the relation between F_L, F_2 and $dF_2/dlnQ^2$ could be violated by non-perturbative contributions, which are expected to be important in the F_L case (see

[11] It must be noted that the cross section of inelastic $c\bar{c}-$ and $b\bar{b}-$pair photoproduction at HERA are described by the BFKL parametrization at a smaller value of Q_0^2 ($Q_0^2 = 1$ GeV^2) [14].

Ref. [50]). The application of present analysis to F_L will give a "non pure" perturbative QCD predictions for the structure function that should be compared with data [41, 43] and with the "pure" perturbative results of Ref. [40].

Acknowledgments

We are grateful to Profs. V.S. Fadin, M. Ciafaloni, I.P. Ginzburg, H. Jung, E.A. Kuraev, L.N. Lipatov and G. Ridolfi for useful discussions. N.P.Z. thanks S.P. Baranov for a careful reading of the manuscript and useful remarks. We thank also to participants of the Workshop "Small x phenomenology" (Lund, March 2001) for the interest in this work and discussions.

One of the authors (A.V.K.) was supported in part by Alexander von Humboldt fellowship and INTAS grant N366. G.P. acknowledges the support of Xunta de Galicia (PGIDT00 PX20615PR) and CICyT (AEN99-0589-C02-02). N.P.Z. also acknowledge the support of Royal Swedish Academy of Sciences.

A Appendix

Here we present the contribution to the amplitude of the DIS process from scalar diagrams [12] in the elastic forward scattering of a photon on a parton. In analogy to Eq. (6) one can represent any one-loop diagram of the elastic forward scattering

$$D_{m_1m_2m_3m_4} \equiv \int \frac{d^Dk_1}{(2\pi)^{D/2}} \, d^{m_1}(k_1)\, d^{m_2}(k-k_1)\, d^{m_3}(q+k_1)\, d^{m_4}(q+k_1-k), \tag{A.1}$$

where $d(k) = (k^2-m^2)^{-1}$, in the form [13]:

$$D_{m_1m_2m_3m_4} = \sum_{n=0}^{\infty} \left(\frac{1}{x}\right)^n \tilde{k}(n) \int_0^{1/(1+4a+b)} dz\; z^{n-1}\beta(z)\tilde{f}_{m_1m_2m_3m_4}(z), \tag{A.2}$$

For application of Eqs. (A.1) and (A.2) to F_2 and F_L coefficient functions, only even n are needed. We choose $\tilde{k}(n)$ so that $\tilde{k}(2n) = 1$.

Below we rewrite Eq. (A.2) in the symbolic form:

$$D_{m_1m_2m_3m_4} \longrightarrow \tilde{k}(n),\; \tilde{f}_{m_1m_2m_3m_4}(z) \tag{A.3}$$

Then, we can represent the needed formulae by:

[12] These diagrams appear after calculation of the traces of diagrams in Fig.1.

[13] This method is very similar to that in Refs. [17, 51] in the case of zero quark masses. Usually the consideration of nonzero masses into Feynman integrals complicates strongly the analysis and requires the use of special techniques (see, for example, Ref. [52]) to evaluate the diagrams. Here it is not the case, the nonzero quark masses only modifies the upper limit of the integral with respect to the Bjorken variable (see the r.h.s. of Eq. (A.2)).

1. The loops:

$$
\begin{aligned}
D_{0110} &\longrightarrow \tilde{k}(n) = 1, && \tilde{f}_{0110}(z) = 1, \\
D_{1001} &\longrightarrow \tilde{k}(n) = (-1)^n, && \tilde{f}_{1001}(z) = 1
\end{aligned} \tag{A.4}
$$

2. The triangles:

$$
\begin{aligned}
D_{1110} &= D_{0111} \longrightarrow \tilde{k}(n) = 1, && \tilde{f}_{1110}(z) = \tilde{f}_{0111}(z) = -z\ f_1(z) \\
D_{1011} &= D_{1101} \longrightarrow \tilde{k}(n) = (-1)^n, && \tilde{f}_{1011}(z) = \tilde{f}_{1101}(z) = -z\ f_1(z)
\end{aligned} \tag{A.5}
$$

3. The boxes:

$$
D_{2110} \longrightarrow \tilde{k}(n) = 1, \qquad \tilde{f}_{0110}(z) = -4z^2\ f_2(z) \tag{A.6}
$$

$$
D_{1111} \longrightarrow \tilde{k}(n) = \frac{(1+(-1)^n)}{2}, \quad \tilde{f}_{1111}(z) = 4z^2\ f_1(z) \tag{A.7}
$$

We would like to note that the result for the second box D_{1111} is very similar to ones for the triangles. In the case of massless quarks this property has been observed in Refs. [17, 51].

B Appendix

We compare the results obtained in Sect. 2 and Appendix A with well known formulae obtained in earlier works (see Refs. [15, 16]).

Following Ref. [16] let us consider the kinematics of virtual $\gamma\gamma$ forward scattering. According to the optical theorem (see Sect. 1) the quantity $F^{\mu\nu\alpha\beta}$ is the absorptive part of the $\gamma\gamma$ forward amplitude, connected with the cross section in the usual way. (The expression of the amplitude in terms of the electromagnetic currents is given in Sect. 1).

In the expansion of $F^{\mu\nu\alpha\beta}$ into invariant functions one should take into account Lorentz invariance, T-invariance (symmetry in the substitution $\mu\nu \leftrightarrow \alpha\beta$) and gauge invariance as well, i.e. [14]

$$
q_1^\mu F^{\mu\nu\alpha\beta} = q_1^\nu F^{\mu\nu\alpha\beta} = q_2^\alpha F^{\mu\nu\alpha\beta} = q_2^\beta F^{\mu\nu\alpha\beta} \tag{B.1}
$$

The tensors in which $F^{\mu\nu\alpha\beta}$ is expanded can be constructed in terms of vectors q_1^μ, q_2^μ and the tensor $g^{\mu\nu}$. In order to take into account explicitly gauge invariance, it is convenient to use their linear combinations:

$$
\mathcal{Q}_1^\mu = \sqrt{\frac{-q_1^2}{\mathcal{X}}}\left[q_2^\mu - q_1^\mu \frac{(q_1 q_2)}{q_1^2}\right], \quad \mathcal{Q}_2^\mu = \sqrt{\frac{-q_2^2}{\mathcal{X}}}\left[q_1^\mu - q_2^\mu \frac{(q_1 q_2)}{q_2^2}\right], \tag{B.2}
$$

$$
R^{\mu\nu} = R^{\nu\mu} = -g^{\mu\nu} + \mathcal{X}^{-1}\Big[(q_1 q_2)(q_1^\mu q_2^\nu + q_1^\nu q_2^\mu) - q_1^2 q_2^\mu q_2^\nu - q_2^2 q_1^\mu q_1^\nu\Big], \tag{B.3}
$$

[14] Sometimes we replace $q \to q_1$ and $k \to q_2$ with the purpose of keeping the symmetry $1 \leftrightarrow 2$ in our formulae in the first part of Appendix B.

where

$$\mathcal{X} = (q_1 q_2)^2 - q_1^2 - q_2^2 \tag{B.4}$$

The unit vectors $\mathcal{Q}_i^\mu$ are orthogonal to the vectors q_i^μ and the symmetrical tensor $R^{\mu\nu}$ is orthogonal both to q_1^μ and q_2^μ, i.e. to $\mathcal{Q}_1^\mu$ and $\mathcal{Q}_2^\mu$:

$$\begin{array}{c} q_1^\mu \mathcal{Q}_1^\mu = q_2^\mu \mathcal{Q}_2^\mu = 0, \quad q_i^\mu R^{\mu\nu} = \mathcal{Q}_i^\mu R^{\mu\nu} = 0, \\ \mathcal{Q}_1^2 = \mathcal{Q}_1^2 = 1, \quad R^{\mu\nu}R^{\mu\nu} = 2, \quad R^{\mu\nu}R^{\nu\rho} = -R^{\mu\rho} \end{array} \tag{B.5}$$

We note, that $R^{\mu\nu}$ is a metric tensor of a subspace which is orthogonal to q_1^μ and q_2^μ. In the c.m.s. of the photons, only two components of $R^{\mu\nu}$ are different from 0 ($R^{xx} = R^{yy} = 1$).

The choice of independent tensors in which the expansion is carried out, has a high degree of arbitrariness. We make this choice so that these tensors are orthogonal to each other, and the invariant functions have a simple physical interpretation:

$$\begin{aligned} F^{\mu\nu\alpha\beta} &= R^{\mu\alpha}R^{\nu\beta}F_{TT} + R^{\mu\alpha}\mathcal{Q}_2^\nu \mathcal{Q}_2^\beta F_{TS} + \mathcal{Q}_1^\mu \mathcal{Q}_1^\alpha R^{\nu\beta}F_{ST} \\ &+ \mathcal{Q}_1^\mu \mathcal{Q}_1^\alpha \mathcal{Q}_2^\nu \mathcal{Q}_2^\beta F_{SS} + \frac{1}{2}\Big[R^{\mu\nu}R^{\alpha\beta} + R^{\mu\beta}R^{\nu\alpha} - R^{\mu\alpha}R^{\nu\beta}\Big]F_{TT}^\tau \\ &- \Big[R^{\mu\nu}\mathcal{Q}_1^\alpha \mathcal{Q}_2^\beta + R^{\mu\beta}\mathcal{Q}_1^\alpha \mathcal{Q}_2^\nu + (\mu\nu \leftrightarrow \alpha\beta)\Big]F_{TS}^\tau \\ &+ \Big[R^{\mu\nu}R^{\alpha\beta} - R^{\mu\beta}R^{\nu\alpha}\Big]F_{TT}^a - \Big[R^{\mu\nu}\mathcal{Q}_1^\alpha \mathcal{Q}_2^\beta - R^{\mu\beta}\mathcal{Q}_1^\alpha \mathcal{Q}_2^\nu + (\mu\nu \leftrightarrow \alpha\beta)\Big]F_{TS}^a \end{aligned} \tag{B.6}$$

The dimensionless invariant functions F_{ab} defined here only depend on the invariants $W^2 = (q_1 + q_2)^2$, q_1^2 and q_2^2. The first four functions are expressed through the cross sections σ_{ab} ($a, b \equiv S, T$ for scalar and transverse photons, respectively). The amplitudes F_{ab}^τ correspond to transitions with spin-flip for each of the photons with total helicity conservation. The last two amplitudes are antisymmetric.

We would like to represent the results of Ref. [15] in terms of our functions, introduced in Section 2.

First of all, we return to the variables introduced in Sect. 2. Then, we have

$$\mathcal{X} \;=\; \frac{Q^4}{4x^2}\tilde{\beta}^2, \quad \mathcal{Q}_1^\mu \;=\; \sqrt{\frac{4bx^2}{Q^2\tilde{\beta}^2}}\Big[q_2^\mu + \frac{1}{2bx}q_1^\mu\Big], \quad \mathcal{Q}_2^\mu \;=\; \sqrt{\frac{4bx^2}{Q^2\tilde{\beta}^2}}\Big[q_1^\mu + \frac{1}{2x}q_2^\mu\Big], \tag{B.7}$$

The results of Ref. [15] have the form [15]:

$$\begin{aligned} \tilde{\beta}F_{TT} &= 4x\beta\Big[1 + 4(a-1-b)T + 12bT^2 - \Big\{1 - 8a^2x^2 + 2(2a-1-b \\ &\qquad +2bx(1 - x(1+b)))T + 24b^2T^2\Big\}f_1 + bx^2 f_2\Big], \\ \tilde{\beta}F_{TS} &= -16x\beta\Big[T - 2x\Big\{ax - b(1 + 2x(a-1-b))T - 6b^2T^2\Big\}f_1 \end{aligned}$$

[15] The original results of Ref. [15] contain an additional factor $[-\pi\alpha^2/Q^2]^{-1}$ in comparison with Eq. (B.8), that has to do with the different normalization used in our article (see Eq. (1)) and in Ref. [16].

$$
\begin{aligned}
&\qquad +bx^2(6a-b+6bT)Tf_2\Big],\\
\tilde\beta F_{ST} &= -16x\beta\Big[T-2x\Big\{ax-(1+x(2a-1-b))T-6b^2T^2\Big\}f_1\\
&\qquad +x^2(6a-b+6bT)Tf_2\Big],\\
\tilde\beta F_{SS} &= 64bxT^2\beta\Big[2-(1+2bx^2)f_1-bx^2f_2\Big],\\
\tilde\beta F^{\tau}_{TT} &= 8x\beta\Big[2aT+(1-a^2)\frac{x^2}{\tilde\beta^2}+6bT^2+x^2\Big\{2(1+a+b)-b-2b(2a-1-b)T\\
&\qquad -12b^2T^2\Big\}f_1\Big],\\
\tilde\beta F^{\tau}_{TS} &= \tilde\beta F^{\tau}_{ST} \;=\; 16b^{1/2}xT\beta\Big[2x-3T+x^2\Big\{2a-1-b+6bT\Big\}f_1\Big],\\
\tilde\beta F^{a}_{TT} &= 4\beta\Big[x-4T+\Big\{2T-x\Big\}f_1-bx^3f_2\Big],\\
\tilde\beta F^{a}_{TS} &= \tilde\beta F^{a}_{ST} \;=\; -16b^{3/2}x^2T\beta\Big[2f_1-f_2\Big],
\end{aligned}
$$

where

$$T=\frac{x(1-x(1+b))}{\tilde\beta^2}$$

Doing the needed projections on Eqs. (B.6) we can express the above functions as combinations of $f^{(1)}$, $f^{(2)}$, $\tilde f^{(1)}$ and $\tilde f^{(2)}$ (see Sect. 2).

$$
\begin{aligned}
\tilde\beta^2F_{SS} &= f^{(1)}, \qquad \tilde\beta^2F_{ST} \;=\; \tilde\beta^2f^{(1)}+\frac{1}{2}f^{(2)}\\
\tilde\beta^2F_{TS} &= \frac{1}{2}\Big[\tilde f^{(2)}-f^{(2)}\Big], \qquad \tilde\beta^2F_{TT} \;=\; \frac{1}{2}\Big[\tilde\beta^2\tilde f^{(1)}-f^{(1)}\Big]
\end{aligned}
\tag{B.8}
$$

The coefficient functions calculated in Sect. 2 can be expressed as combinations of F_{AB} $(A,B=S,T)$.

For non interacting gluons:

$$
\begin{aligned}
\tilde\beta^2C_2 &= \mathcal{K}\left[F_{SS}+F_{ST}-2(F_{TT}+F_{TS})\right],\\
\tilde\beta^2C_L &= \mathcal{K}\left[F_{SS}-2F_{TS}+4bx^2\Big(F_{ST}-2F_{TT}\Big)\right]
\end{aligned}
\tag{B.9}
$$

For the BFKL projector:

$$
\begin{aligned}
\tilde\beta^4C_{2,BFKL} &= \mathcal{K}\left[F_{SS}+F_{ST}+F_{TS}+F_{TT}\right],\\
\tilde\beta^4C_{L,BFKL} &= \mathcal{K}\left[F_{SS}+F_{TS}+4bx^2\Big(F_{ST}+F_{TT}\Big)\right]
\end{aligned}
\tag{B.10}
$$

C Appendix

Here we consider the particular cases: $k^2 = 0$, $m^2 = 0$ and $Q^2 \to 0$ which are relevant to compare with others.

C.1 The case $k^2 = 0$

When $k^2 = 0$

$$C_2^g(x) \;=\; \mathcal{K}\, \left[f^{(1)} + \frac{3}{2}\, f^{(2)}\right] \quad \text{and} \quad C_L^g(x) \;=\; \mathcal{K}\, f^{(2)} \tag{C.1}$$

with

$$f^{(1)} \;=\; -2\,\beta\Bigg[\Big(1-2x(1-x)(1-2a)\Big) - \Big(1-2x(1-2a)+2x^2(1-4a^2)\Big) \\ L(\beta)\Bigg] \tag{C.2}$$

$$f^{(2)} \;=\; 8x\,\beta\Bigg[(1-x) - 2xa\; L(\beta)\Bigg], \tag{C.3}$$

where

$$\beta^2 = 1 - \frac{4ax}{(1-x)}$$

and the function $L(\beta)$ has been defined in Eq. (36).

Equations (C.1)-(C.3) coincide with the results of Ref. [53].

Indeed, we have

$$C_2^g \;=\; \mathcal{K}\,(-2)\beta\Bigg[\Big(1-4x(2-a)(1-x)\Big) \\ - \;\Big(1-2x(1-2a)+2x^2(1-6a-4a^2)\Big)\; L(\beta)\Bigg] \tag{C.4}$$

$$C_L^g \;=\; \mathcal{K}\; 8x\beta\Bigg[(1-x) - 2xa\; L(\beta)\Bigg] \tag{C.5}$$

The consideration of the BFKL projector does not change the results given above because the additional terms (see Eq. (31)) are proportional to k^2 and they are negligible. The expression in Eq. (C.5) also coincides with the corresponding result in Ref. [25] (see Eqs. (A17,A18)).

C.2 The case $m^2 = 0$

When $m^2 = 0$ the coefficient functions $C_k^g(x)$ are defined through $f^{(1)}$ and $f^{(2)}$ (see Eqs. (20), (21)) being in this case

$$f^{(1)} \;=\; -2\Bigg[2 - \Big(1-2x(1+b)+2x^2(1+b)^2\Big)\; L(\tilde{\beta})\Bigg] \tag{C.6}$$

$$f^{(2)} \;=\; 8x(1+b)(1-(1+b)x)\Big[1-2bx^2\;L(\tilde\beta)\Big] \tag{C.7}$$

For the coefficient functions themselves, we have

$$\begin{aligned}
\tilde\beta^4\;C_2^g &= \mathcal{K}\,(-2)\,(1-x(1+b))\Bigg[2\Bigg(1-2x(1+b)+\frac{x^2(1-b)^2}{1-x(1+b)}\Bigg)\\
&- \Bigg(1-x(1+b)-4x^3b(1+b)+\frac{x^2(1-b)^2}{1-x(1+b)}\Bigg)\;L(\tilde\beta)\Bigg] \qquad (C.8)\\
\tilde\beta^4\;C_L^g &= \mathcal{K}\,8x\,(1-x(1+b))\Bigg[\Bigg((1+b)-2bx\Bigg[1+\frac{x^2(1-b)^2}{1-x(1+b)}\Bigg]\Bigg)\\
&+ bx\Bigg(1-3x(1+b)+4x^3b(1+b)+\frac{x^2(1-b)^2}{1-x(1+b)}\Bigg)\;L(\tilde\beta)\Bigg] \qquad (C.9)
\end{aligned}$$

In the case of the BFKL projector, the coefficient functions $C_k^g(x)$ are defined by Eqs. (C.1), (23) and (24) with the replacement $f^{(i)} \to f^{(i)}_{BFKL}$ as in Eq. (32). In Eq. (32) the expressions for $f^{(i)}$ can be found in Eqs. (C.6), (C.7) while for $\tilde f^{(i)}$ are given by:

$$\tilde f^{(1)} \;=\; -\frac{(1+b)(1-x(1+b))}{bx}\Big[1-2bx^2\;L(\tilde\beta)\Big] = -\frac{1}{8bx^2}f^{(2)} \tag{C.10}$$

$$\tilde f^{(2)} \;=\; 4(1-x(1+b))^2\Big[3-(1+2bx^2)\;L(\tilde\beta)\Big] \tag{C.11}$$

and, thus,

$$f^{(1)}_{BFKL} \;=\; C_2^g/\mathcal{K} \tag{C.12}$$

$$\begin{aligned}
\tilde\beta^4\;f^{(2)}_{BFKL} &= 8x(1-x(1+b))\Big[1+b-18bx(1-x(1+b))\\
&+ 2bx\,\Big(3-4x(1+b)+6bx^2(1-x(1+b))\Big)\;L(\tilde\beta)\Big] \qquad (C.13)
\end{aligned}$$

For the coefficient functions $C^g_{k,BFKL}(x)$ we have the following results:

$$\begin{aligned}
\tilde\beta^8\;C^g_{2,BFKL} &= \mathcal{K}\,(-2)\,(1-x(1+b))\Bigg[2\Bigg(1-5x(1+b)\\
&+ x^2(1+48b+b^2)+x^3(1+b)(1-48b+b^2)+\frac{x^4(1-b)^4}{1-x(1+b)}\Bigg)\\
&- \Bigg(1-x(1+b)+(1-30b+b^2)x^2+(1-50b+b^2)x^3(1+b)\\
&+ 72x^4b^2-56x^5b^2(1+b)+\frac{x^4(1-b)^4}{1-x(1+b)}\Bigg)\;L(\tilde\beta)\Bigg] \qquad (C.14)
\end{aligned}$$

$$
\begin{aligned}
\tilde{\beta}^8\, C^g_{L,BFKL} &= \mathcal{K}\, 8x\,(1-x(1+b))\Bigg[\Big((1+b)-20bx+24b(1+b)x^2 \\
&- 2b(1+12b+b^2)x^3-2(1+b)b(1-12b+b^2)x^4-2bx\,\frac{x^4(1-b)^4}{1-x(1+b)}\Big) \\
&+ bx\Big(7-11x(1+b)+(1-42b+b^2)x^2+(1-30b+b^2)(1+b)x^3 \\
&+ 24b^2x^4-8b^2(1+b)x^5+\frac{x^4(1-b)^4}{1-x(1+b)}\Big)\,L(\tilde{\beta})\Bigg] \qquad \text{(C.15)}
\end{aligned}
$$

C.3 The case $Q^2 \to 0$

Using the definitions in Eq. (35), when $x \to 0$ we have got the following relations (at $O(x)$):

for the intermediate functions:

$$
\begin{aligned}
\tilde{\beta}^2 &= 1-4x\Delta, \quad \beta^2=\hat{\beta}^2(1-4\gamma x), \\
f_1 &= L(\hat{\beta})\,(1+2x(\gamma+\Delta))-2x(\gamma+\Delta)\frac{(1-\Delta)}{z}, \\
f_2 &= -\frac{2(1-\Delta)}{z}\Big[1-2x\frac{1-\Delta-2z}{z}\,(\gamma+\Delta)\Big], \qquad \text{(C.16)}
\end{aligned}
$$

where

$$
z=\frac{\rho}{2}, \quad \gamma=\frac{z/2}{(1-\Delta)(1-\Delta-2z)}
$$

for the basic functions:

$$
\begin{aligned}
f^{(1)} &= -2\hat{\beta}\Bigg[1-2(1-\Delta)(\Delta-z)-\Big(1-2(1-\Delta)\Delta+2(1-z)z\Big)L(\hat{\beta}) \\
&+ 2x\Bigg\{\frac{1-\Delta}{z}\,(\Delta+(\Delta-z)(1-2z\Delta))-\frac{1-\Delta-z}{z}\,\gamma \\
&+ \Big(1-\Delta\Big[3-2(1-\Delta)\Delta+2(1-z)z\Big]\Big)L(\hat{\beta})\Bigg\}\Bigg], \qquad \text{(C.17)} \\
f^{(2)} &= 8x\hat{\beta}\Bigg[(1-\Delta)\left(1-2\frac{\Delta(1-\Delta)}{z}(z-\Delta)\right)-\Big(2\Delta^2(1-\Delta) \\
&+ z(1-2\Delta(1-\Delta))\Big)L(\hat{\beta})\Bigg], \\
x\tilde{f}^{(1)} &= -\hat{\beta}\Bigg[\Big\{(1-\Delta)-x(3-6\Delta+4\Delta^2)\Big\}-\Big\{z+2x(\Delta(1-\Delta)-z)\Big\}L(\hat{\beta})\Bigg], \\
x\tilde{f}^{(2)} &= 4x\hat{\beta}(1-\Delta)^2\Big[2-L(\hat{\beta})\Big], \qquad \text{(C.18)}
\end{aligned}
$$

and, thus,

$$
f^{(1)}_{BFKL} = f^{(1)} + 4\hat{\beta}\Delta\Bigg[3\Big(1-\Delta-zL(\hat{\beta})\Big)-x\Bigg\{11-46\Delta+40\Delta^2+4z(1-\Delta)
$$

$$- \; 2\Big[1-5(1-\Delta)\Delta+z(5-2z-12\Delta)\Big]\Big\}L(\hat\beta)\Big], \tag{C.19}$$

$$f^{(2)}_{BFKL} \; = \; f^{(2)} \; - \; 48x\hat\beta\Delta(1-\Delta)\Big[2-L(\hat\beta)\Big]. \tag{C.20}$$

Similarly to Eq. (C.18), the coefficient functions in Eq. (39) and the functions $f^{(1)}_{BFKL}$ in Eq. (40) have the additional terms proportional x.

$$\begin{aligned} C^g_2/\mathcal{K} \; &= \; f^{(1)} \; + \; 4x\hat\beta\Big[6\,\frac{\Delta^2(1-\Delta)^2}{z}+3-\Delta\Big(11-16\Delta+10\Delta^2+4z(1-\Delta)\Big) \\ &+ \; \Big\{2\Delta\Big[1-5(1-\Delta)\Delta+z(5-2z-3\Delta)\Big]-3z\Big\}L(\hat\beta)\Big], \end{aligned} \tag{C.21}$$

$$\begin{aligned} C^g_L/\mathcal{K} \; &= \; 8x\hat\beta\Big[2\,\frac{\Delta^2(1-\Delta)^2}{z}+1-2\Delta\Big(2-3\Delta+2\Delta^2+z(1-\Delta)\Big) \\ &+ \; \Big\{\Delta\Big[1-4(1-\Delta)\Delta+2z(2-z-\Delta)\Big]-z\Big\}L(\hat\beta)\Big], \end{aligned} \tag{C.22}$$

$$\begin{aligned} C^g_{2,BFKL}/\mathcal{K} \; &= \; C^g_2/\mathcal{K} \; + \; 4\hat\beta\Delta\Big[3\Big(1-\Delta-zL(\hat\beta)\Big)-x\Big\{47-130\Delta+88\Delta^2 \\ &+ \; 4z(1-\Delta)-2\Big[10-23\Delta+14\Delta^2+z(5-2z-18\Delta)\Big]L(\hat\beta)\Big\}\Big], \end{aligned} \tag{C.23}$$

$$C^g_{L,BFKL}/\mathcal{K} \; = \; C^g_L/\mathcal{K} \; - \; 48x\hat\beta\Delta\Big[(1-\Delta)(2-3\Delta)-\Big[(1-\Delta)^2-z\Delta\Big]L(\hat\beta)\Big] \tag{C.24}$$

References

[1] H1 Collab.: S. Aid et al., Z. Phys. **C72** (1996) 593; Nucl. Phys. **B545** (1999) 21.

[2] ZEUS Collab.: J. Breitweg et al., Phys. Lett. **B407** (1997)402.

[3] ZEUS Collab.: J. Breitweg et al., Eur. Phys. J. **C12** (2000) 35.

[4] H1 Collab.: S. Adloff et al., Paper submitted to ICHEP2000, Osaka, Japan, Abstract 984.

[5] EM Collab.: J.J. Aubert et al., Nucl. Phys. **B213** (1983) 31; Phys. Lett. **B94** (1980) 96; **B110** (1983) 72.

[6] A.M. Cooper-Sarkar, R.C.E. Devenish and A. De Roeck, Int. J. Mod. Phys. **A13** (1998) 3385.

[7] V.N. Gribov and L.N. Lipatov, Sov. J. Nucl. Phys. **18** (1972) 438, 675.

[8] L.N. Lipatov, Sov. J. Nucl. Phys. **20** (1975) 93;
G. Altarelli and G. Parisi, Nucl. Phys. **B126** (1977) 298;
Yu.L. Dokshitzer, Sov. Phys. JETP **46** (1977) 641.

[9] B.A. Kniehl et al., Z. Phys. **C76** (1997) 689;
J. Binnewies et al., Z. Phys. **C76** (1997) 677;
M. Cacciari et al., Phys. Rev. **D55** (1997) 2736, 7134.

[10] S. Frixione et al., Phys. Lett. **B348** (1995) 653, Nucl. Phys. **B454** (1995) 3.

[11] M.A.G. Aivazis et al., Phys. Rev. **D50** (1994) 3102.

[12] L.N. Lipatov, Sov. J. Nucl. Phys. **23** (1976) 642;
E.A. Kuraev, L.N. Lipatov and V.S. Fadin, Sov. Phys. JETP **44** (1976) 45, **45** (1977) 199;
Ya.Ya. Balitzki and L.N. Lipatov, Sov. J. Nucl. Phys. **28** (1978) 822;
L.N. Lipatov, Sov. Phys. JETP **63** (1986) 904.

[13] J. Kwiecinski, Acta Phys. Polon. **B27** (1996) 3455.

[14] A. V. Lipatov and N.P. Zotov, Mod. Phys. Lett. **A15** (2000) 695;
A. V. Lipatov, V.A. Saleev and N.P. Zotov, Mod. Phys. Lett. **A15** (2000) 1727.

[15] V.N. Baier, V.S. Fadin and V.A. Khose, JETP **50** (1966) 156 (in Russian);
V.N. Baier, V.M. Katkov and V.S. Fadin, *Relativistic electron radiation*, (Moscow, Atomizdat, 1973) (in Russian);
V.G. Zima, Yad. Fiz. **16** (1972) 1051.

[16] V.M. Budnev, I.F. Ginsburg, G.V. Meledin and V.G. Serbo, Phys. Rept. **15** (1975) 181.

[17] D.I. Kazakov and A.V. Kotikov, Theor.Math.Phys. **73** (1987) 1264; Nucl.Phys. **B307** (1988) 721; E: **B345** (1990) 299.

[18] R.K. Ellis, W. Furmanski, and R. Petronzio, Nucl. Phys. **B207** (1982) 1; **B212** (1983) 29.

[19] S. Catani, M. Ciafaloni and F. Hautmann, Phys. Lett. **B242** (1990) 97; Nucl. Phys. **B366** (1991) 135.

[20] J.C. Collins and R.K. Ellis, Nucl. Phys. **B360** (1991) 3.

[21] E.M. Levin, M.G. Ryskin, Yu.M. Shabelskii and A.G. Shuvaev, Sov. J. Nucl. Phys. **53** (1991) 657.

[22] E.A. Kuraev and L.N. Lipatov, Sov. J. Nucl. Phys. **16** (1973) 584.

[23] W. Vogelsang, Z. Phys. **C50** (1991) 275;
A. Gabrieli and G. Ridolfi, Phys. Lett. **B417** (1998) 369.

[24] G. Bottazzi, G. Marchesini, G.P. Salam, and M. Scorletti, JHEP **9812** (1998) 011.

[25] S. Catani, M. Ciafaloni, and F. Hautmann, Preprint CERN - TH.6398/92, in Proceeding of the Workshop on Physics at HERA (Hamburg, 1991), v.2, p.690.

[26] M.G. Ryskin and Yu.M. Shabelski, Z. Phys. **C61** (1994) 517; **C66** (1995) 151.

[27] J. Blumlein, Preprint DESY 95-121 (hep-ph/9506203).

[28] M. Gluck, E. Reya, and A. Vogt, Z. Phys. **C67** (1995) 433.

[29] V.N. Fadin and L.N. Lipatov, Phys. Lett. **B429** (1998) 127;
M. Ciafaloni and G. Camici, Phys. Lett. **B430** (1998) 349.

[30] A.V. Kotikov and L.N. Lipatov, Nucl. Phys. **B582** (2000) 19.

[31] D.A. Ross, Phys. Lett **B431** (1998) 161.

[32] G. Salam. JHEP **9807** (1998) 019; Acta Phys.Polon. **B30** (1999) 3679

[33] S.J. Brodsky, V.S. Fadin, V.T. Kim, L.N. Lipatov, and G.B. Pivovarov, JETP Lett. **70** (1999) 155.

[34] S. P. Baranov and N.P. Zotov, Phys. Lett. **B458** (1999) 389.

[35] N.N. Nikolaev and B.G. Zakharov, Phys. Lett **B333** (1994) 250; Phys. Lett **B327** (1994) 157;
J. Kwiecinski, A.D. Martin, and P.J. Sutton, Z. Phys. **C71** (1996) 585;
B. Andersson, G. Gustafson, H. Kharrazina, and J. Samuelsson, Z. Phys. **C71** (1996) 613;
N.N. Nikolaev and V.R. Zoller, *in* Proc. QCD-2000, Villefranche-sur-Mer, January 2000 (hep-ph/0001084);
B.I. Ermolaev, M. Greco, and S.I. Troyan, Nucl.Phys. **B594** (2001) 71.

[36] L3 Collaboration, M. Acciarri et al., Phys. Lett. **B453** (1999) 333;
M. Kienzle, talk given at the International Symposium on Evolution Equations and Large Order Estimates in QCD, Gatchina, Russia, May,2000.

[37] A.V. Lipatov and N.P. Zotov, *in* Proc. of the 8th Int. Workshop on Deep Inelastic Scattering, DIS 2000 (2000), World Scientific, p. 157.

[38] A.V. Kotikov and G. Parente, Nucl. Phys. **B549** (1999) 242; Nucl. Phys. (Proc. Suppl.) **99** (2001) 196; *in* Proc. of the Int. Conference PQFT98 (1998), Dubna (hep-ph/9810223); *in* Proc. of the 8th Int. Workshop on Deep Inelastic Scattering, DIS 2000 (2000), Liverpool, p. 198 (hep-ph/0006197).

[39] A.V. Kotikov and G. Parente, *in* Proc. Int. Seminar Relativistic Nuclear Physics and Quantum Chromodynamics (2000), Dubna (hep-ph/0012299); *in* Proc. of the 9th Int. Workshop on Deep Inelastic Scattering, DIS 2001 (2001), Bologna (hep-ph/0106175).

[40] A.V. Kotikov, JETP **80** (1995) 979;
A.V. Kotikov and G. Parente, *in* Proc. Int. Workshop on Deep Inelastic Scattering and Related Phenomena (1996), Rome, p. 237 (hep-ph/9608409); Mod. Phys. Lett. **A12** (1997) 963; JETP **85** (1997) 17; hep-ph/9609439.

[41] H1 Collab.: S. Aid et al., Phys.Lett. **B393** (1997) 452;
H1 Collab.: D. Eckstein, *in* Proc. Int. Workshop on Deep Inelastic Scattering, (2001), Bologna;
H1 Collab.: M.Klein, *in* Proc. of the 9th Int. Workshop on Deep Inelastic Scattering, DIS 2001 (2001), Bologna.

[42] R.S. Thorne, Phys.Lett. **B418** (1998) 371.

[43] CCFR/NuTeV Collab.: U.K. Yang et al., *in* Proc. Int. Conference on High Energy Physics (2000) Osaka, Japan (hep-ex/0010001);
CCFR/NuTeV Collab.: A. Bodek, *in* Proc. of the 9th Int. Workshop on Deep Inelastic Scattering, DIS 2001 (2001), Bologna (hep-ex/00105067).

[44] S. Keller, M. Miramontes, G. Parente, J. Sánchez-Guillén, and O.A. Sampayo, Phys.Lett. **B270** (1990) 61;
L.H. Orr and W.J. Stirling, Phys.Rev.Lett. **B66** (1991) 1673;
E. Berger and R. Meng, Phys.Lett. **B304** (1993) 318;
A.V. Kotikov, JETP Lett. **59** (1994) 1; Phys.Lett. **B338** (1994) 349.

[45] H. Jung, Nucl. Phys. (Proc. Suppl.) **79** (1999) 429.

[46] G. Wolf, Preprint DESY 01-058 (hep-ex/0105055);
L. Gladilin and I. Redoldo, to appear in “The THERA Book” (hep-ph/0105126).

[47] M.A. Kimber, A.D. Martin, and M.G. Ryskin, Phys. Rev. **D63** (2001) 114027.

[48] A.M. Cooper-Sarkar, G. Ingelman, R.G. Roberts and D.H. Saxon, Z. Phys. **C39** (1988) 281;
A.V. Kotikov, Phys. Atom. Nucl. **57** (1994) 133; Phys. Rev. **D49** (1994) 5746.

[49] K. Prytz, Phys.Lett. **B311** (1993) 286;
A.V. Kotikov, JETP Lett. **59** (1994) 667;
A.V. Kotikov and G. Parente, Phys.Lett. **B379** (1996) 195.

[50] J. Bartels, K.Golec-Biernat, and K. Peters, Eur.Phys.J. **C17** (2000) 121.

[51] A.V. Kotikov, Theor.Math.Phys. **78** (1989) 134.

[52] A.V. Kotikov, Phys.Lett. **B254** (1991) 158; **B259** (1991) 314; **B267** (1991) 123.

[53] E. Witten, Nucl. Phys. **B104** (1976) 445;
M. Gluck and E. Reya, Phys. Lett. **B83** (1979) 98;
F.M. Steffens, W. Melnitchouk, and A.W. Thomas, Eur.Phys.J. **C11** (1999) 673.